ENTE PER LE NUOVE TECNOLOGIE, L'ENERGIA E L'AMBIENTE

Associazione ENEA-EURATOM sulla Fusione

FUSION UNIT
FUSION TECHNOLOGIES

TITLE

Support to the ITER Diagnostic Design: Wide-Angle Viewing System to Supplement Other Diagnostics

Second Intermediate report

AUTORE

G. Maddaluno

Reference:

EFDA Contract 03-1113

DATA

February 2005

VISIBLE/IR SPECTROSCOPIC ANALYSIS

The particle flux density can be inferred from the emission line radiance

$$\Phi \text{ [particles/m}^2\text{/s]} = 4\,\Pi\,(S / X\,B)\,R \qquad (1)$$

with S = ionisation rate [m^3/s]

X = excitation rate [m^3/s]

B = branching ratio of the observed line

R = radiance [phot. /s/m^2/ster]

For minimum deuterium flux density to be measured $\Phi = 10^{18}$ particles/m^2/s [1] we get $R_{H_\alpha} = 5 \cdot 10^{15}$ phot. /s/m^2/ster.

This means, according to (1), $(S / X\,B)_{H_\alpha} \sim 16$, a value that can result from regimes of very low temperature, high density

or high temperature and low-medium density. In Fig. 1 the value of (S / X B) H_α as a function of the electron temperature is reported for three values of the plasma density [2].

Fig. 1

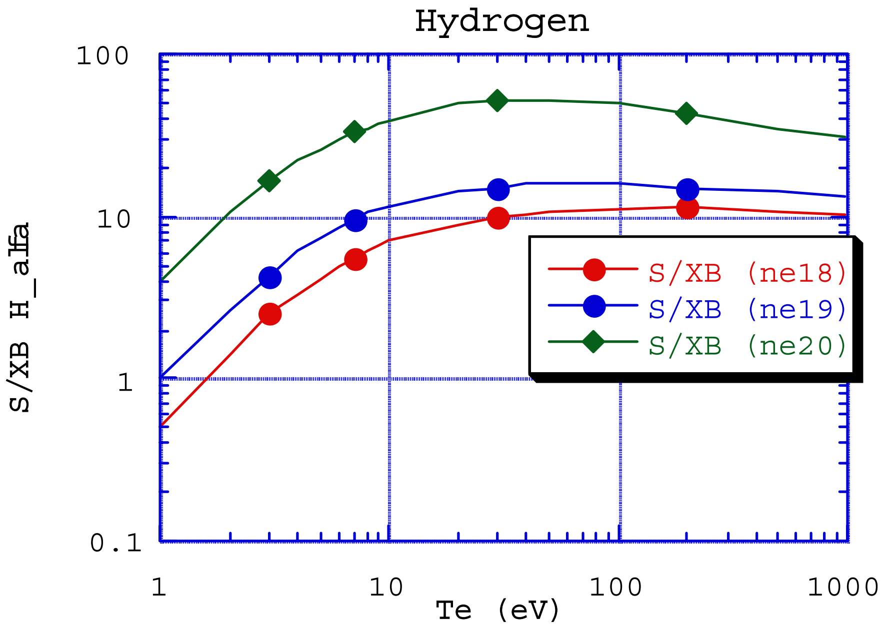

The number of photons/s arriving to the detector is given by:

$$\Phi \text{ (photons/s)} = T \cdot E \cdot R \qquad (2)$$

where T and E are the transmission and the etendue $[m^2 \cdot \text{ster}]$ of the system, respectively.

For the H_a spectroscopy optical systems the etendue is foreseen to be $2.5 \div 5.2 \cdot 10^{-8}$ and the total transmission $.75 \div 1.0 \cdot 10^{-3}$ [1].

Therefore the number of photons/s arriving to the detector is expected to be:

$$\Phi \text{ (photons/s)} = (0.94 \div 2.6) \cdot 10^5$$

It means $(0.94 \div 2.6) \cdot 10^2$ photons/ms, to be compared with the typical lower limit of the number of photons that can be detected on existing machines ($= 1.0 \cdot 10^3$ photons/ms) [3]. Therefore for the H_a spectroscopy optical systems the detection of the expected minimum deuterium flux density seems rather difficult. In the same way, allowing for a similar transmission of $1.0 \cdot 10^{-3}$, the etendue of the IR-TV system must be not lower than about 10^{-7}.

As far as the impurity fluxes are concerned, we can estimate, for example, how large the system etendue should be in order to detect the minimum foreseen tungsten influx, i.e. 4×10^{14} atoms/s [4]. By considering, in a pessimistic way, that the tungsten influx is homogeneous all around the vacuum vessel we get a tungsten density flux of $4 \times 10^{14} / 678 = 5.9 \times 10^{11}$ atoms /m^2/s, 678 m^2 being the plasma suface area. For a typical value of the ratio (S / X B) for the W I line (= 16, [5]), we get a radiance R = $2.9\ 10^9$ phot. /s/m^2/ster. By still allowing for a transmission of $1.0 \cdot 10^{-3}$ we see that in this case we need an etendue value of at least 3×10^{-1}.

The field of view of the visible channel being the same of the infrared channel (therefore including material surfaces), the contribution of the thermal emission from heated first wall to the detector signal is also to be evaluated.

The number of photons/m^2/sec emitted by a surface at temperature T, emissivity $\varepsilon = 1$, FOV = Π, in a 100 nm wide wavelength range $\Delta\lambda$ around H_α ($.6 \div .7$ m) is about:

$N = 1.98 \cdot 10^{8}$ for $T = 500$ °K

$N = 3.35 \cdot 10^{17}$ for $T = 1000$ °K

$N = 4.50 \cdot 10^{20}$ for $T = 1500$ °K

$N = 1.70 \cdot 10^{22}$ for $T = 2000$ °K

It can be seen that, for T about 1000 °K, H_α measurements are difficult with large wavelength range. Narrow filters can be used (as is normally done in spectroscopic measurements); i.e., with $\Delta\lambda = 10$ nm, $N = 3.06 \cdot 10^{16}$, or H_{β}, instead of H_α measurements can be carried out, as suggested in ref. [1]. In effect, between 0.481 and 0.491 μ, the number of photons/m^2/sec emitted by a surface at temperature T = 1000 °K is $N = 4.78 \cdot 10^{13}$, i.e. about 4 orders of magnitude less than between 0.6 and 0.7 μ, while $(S / X\,B)_{H\beta} \sim 10 \cdot (S / X\,B)_{H\alpha}$ so that $R_\beta \sim R_\alpha / 10$ (i.e. only a factor 10 less). In Fig. 2 and 3 the value of $(S / X\,B)_{H\beta}$ as a function of the electron temperature, for several values of the plasma density, and as a function of the plasma density at Te = 30 eV, respectively, is reported [2].

Fig. 2

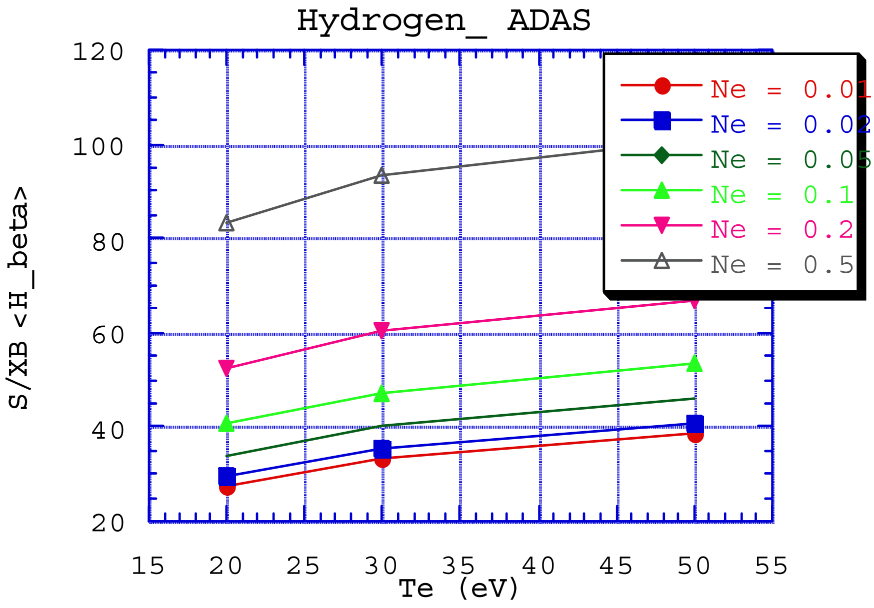

Fig. 3

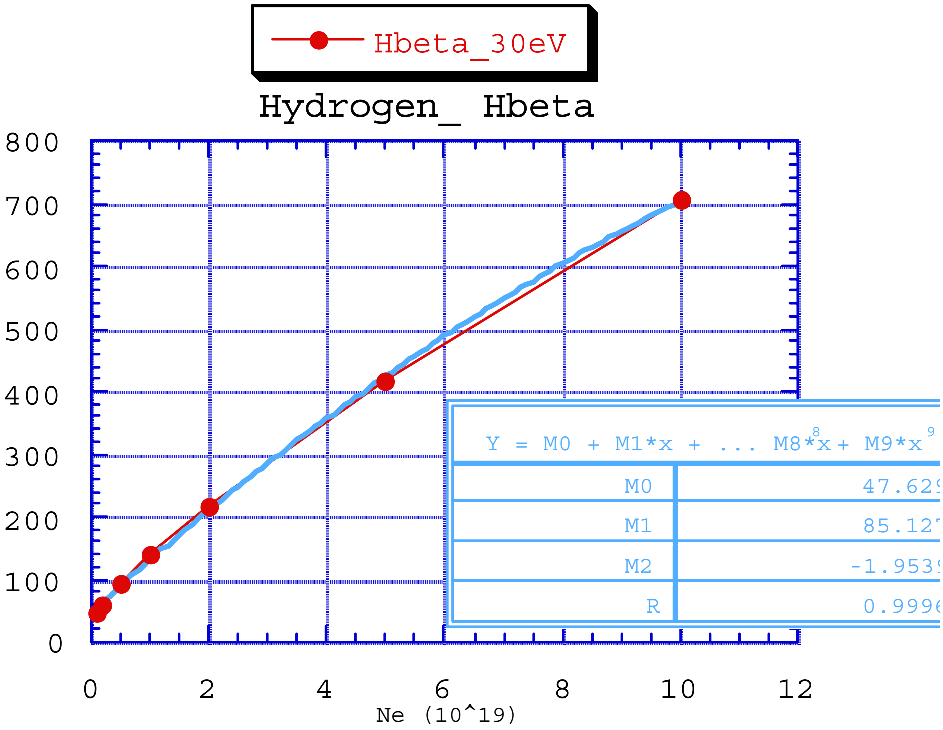
Hbeta_30eV
Hydrogen_ Hbeta
800
700
600
500
400
300
200
100
0
0
2
4
6
8
10
12
Ne (10^19)
Y = M0 + M1*x + ... M8*x^8 + M9*x^9
M0
47.62
M1
85.12
M2
-1.953
R
0.999

In-vessel inspection

In order to assess to which extent the system can be used for first-wall damage localisation and assessment, maintenance and localisation of remote handling tools, we must evaluate the MTF (Modulation Transfer Function) of the complex endoscope-CCD, which establishes the system capability of reproduce the contrast existing on object plane. In other words, the plot of this function versus cycles/mm provides information on the spatial resolution the complex endoscope-CCD can achieve.

According to Rayleigh criterion of image resolution, two point sources, on the object plane, that result in two spots on the CCD plane with barycentre separated by a distance minor or equal to the pixel pitch p, can be spatially resolved by the optical system (endoscope + CCD). Assuming that the endoscope is nearly diffraction limited, the matching between endoscope and CCD is optimum when: $R_{84\%} \leq p$.

Here $R_{84\%}$ is the maximum value the radius $r_{84\%} = 1.22\ \lambda\ f/\#$ (diffraction limit [4]) assumes when the point source is varying in all the F.O.V. and f/# is the endoscope f-number.

This relation can be written as $0.41\ \nu_0 \geq \nu_{CCD}$

where $\nu_0 = 1 / \lambda\ f/\#$ is the endoscope cut-off frequency and $\nu_{CCD} = 1 / 2p$ is CCD cut-off frequency.

By using formula for monochromatic MTF [5]:

$$\mathrm{MTF}(\upsilon) = \begin{cases} \dfrac{2}{\pi}\left[\cos^{-1}\left(\dfrac{\upsilon}{\upsilon_0}\right) - \dfrac{\upsilon}{\upsilon_0}\sqrt{1-\left(\dfrac{\upsilon}{\upsilon_0}\right)^2}\ \right] & \text{per } 0 < \upsilon < \upsilon_0 \\ \\ 0 & \text{per } \upsilon > \upsilon_0 \end{cases}$$

and by allowing for 0.5 being an MTF value providing a good contrast reproduction, it is possible to find that

the optimum matching between endoscope and CCD is reached when the endoscope MTF at $\nu = \nu_{CCD}$ is MTF $\nu_{CCD} \geq 0.5$.

By using a CCD with the pixel pitch p =10 μm, we get that the endoscope MTF must be $\geq$ 0.5 at 50 cycles/mm. In principle this performance can be reached for an endoscope working in both IR and visible wavelength. As a matter of the fact the refractive IR/visible endoscope designed by ENEA for JET-EP [6] satisfies this condition. In fig. 4 the MTF for JET-EP endoscope visible channel and in Table 1 , columns 2 and 3, the minimum x and y object dimension that can be resolved by the endoscope – FPA (or CCD) system are reported.

To get resolution improvement by reducing the CCD pixel pitch, we need also to decrease the endoscope f-number. In fact, from the diffraction limit formula, smaller the f-number and smaller the radius of the spot on the CCD plane the energy is focused within. At a fixed focal distance, reducing the endoscope f-number means to increase the numerical aperture in the object plane and this is heavily conditioned by geometrical constrains. Moreover it should be taken into account that the visible spatial resolution for JET-EP endoscope was achieved with a 100 nm wide wavelength range: the utilization of the endoscope for in-vessel inspection requires a larger bandwidth, with consequent degradation of the spatial resolution due to chromatic aberrations. It seems reasonable for ITER endoscope to foresee a spatial resolution not better than the one achieved in the ENEA JET-EP endoscope design, i.e. about 10 mm. This resolution is lower than the one required for in-vessel inspection: nevertheless it could be still sufficient for shot by shot inspection as long as idoneous illumination can be guaranteed. As far as this last point, we should consider that for a visible inspection between shots any light source must be necessarily provided from the outside of the vacuum chamber through equatorial or vertical ports. How large the intensity of this light must be, in order to take advantage of all the capability of the endoscope in reproducing the contrast of the scene? We can calculate this intensity by considering the minimum illumination we need in every point of the field of view in order to allow for a photopic vision of the scene (maximum sensitivity at λ=0.555μm). The illumination in a point P of an elemental surface dA, provided by a point source S, with luminous intensity I, at distance R, is given by E= $d\phi$ / dA where $d\phi$ is the light flux, emitted by the source S, incident on the surface dA. The light flux $d\phi$ is equal to the light flux emitted by the source in the solid angle $d\Omega = dA \cos\theta / R^2$, that is $d\phi = I_\theta \, d\Omega = I_\theta \, dA \cos\theta / R^2$ where θ is the angle between the R direction and the normal to the surface. I_θ is the light intensity in the direction defined by θ angle, i.e. the amount of light flux emitted within the solid angle centred around that direction. If the source is not isotropic, its photometric curve, relevant to the plane passing through S and P, is to be known. Then the illumination E is given by $E = I_\theta \cos\theta / R^2$. From this we can calculate, within the field of view, how large the light intensity must be, in order to provide the minimum required illumination in every point of the scene, irrespective of the surface orientation.

Fig. 4

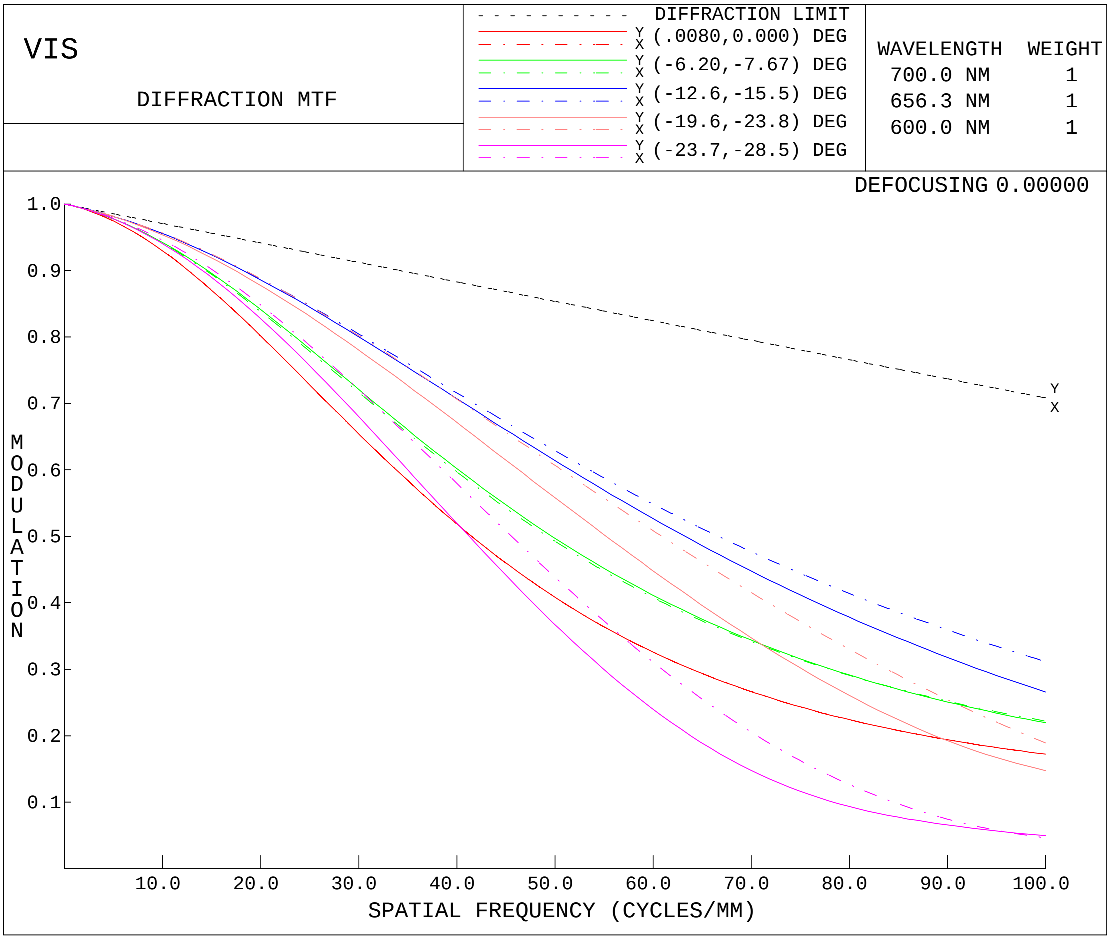

Tab. 1

F.O.V.	**Pixel x-dimension**	**Pixel y-dimension**	**Reduction factor x**	**Reduction factor y**	**r_{84} % (μm) (shift=**	**r_{84} % (μm) (shift=**
0°	5.3	5.3	0.190	0.190	10	10
10°	5.4	5.5	0.184	0.183	9	8
20°	6.0	6.2	0.167	0.162	7	7
30°	7.0	7.5	0.143	0.133	6	8
35°	7.7	8.5	0.129	0.117	8	11

References

[1] N 55 DDD 5 01-07-23 W 0.4 Design Description Document – Diagnostics – 5.5.E Spectroscopic and NPA Systems

[2] G. Apruzzese, private communication

[3] T. Sugie et al.,30th EPS, Vol. 27A, P-4.63

[4] M. Born and E. Wolf, “Principles of optics”, Cambridge University Press, pp. 439-443, (1999)

[5] C.S. Williams and O:A: Becklund, “Introduction to the Optical transfer Function”, John Wiley&Sons, p. 154 (1989)

[6] G. Maddaluno, V. Greco, “Wide Angle Infrared Endoscope And IR Camera Specifications”, Contract EFDA 02/680 – Final Report (June 2003)